J. Electrochem. Sci. Eng. **14(3)** (2024) 369-382; http://dx.doi.org/10.5599/jese.2253

Open Access : : ISSN 1847-9286
https://pub.iapchem.org/ojs/index.php/JESE

Original scientific paper

Optimal design of $LiMn_2O_4$ for high-rate applications by means of citric acid aided route and microwave heating

Yurii V. Shmatok[1,✉], Hanna V. Potapenko[1,2] and Sviatoslav A. Kirillov[1]

[1]*Joint Department of Electrochemical Energy Systems of the National Academy of Science of Ukraine, 38A Vernadsky Ave., 03680 Kyiv, Ukraine*

[2]*Faculty of Materials Metallurgy and Chemistry, Jiangxi University of Science and Technology, Ganzhou 341000, China*

Corresponding author: ✉ yu.shmatok@gmail.com

Received: January 24, 2024; Accepted: June 11, 2024; Published: June 13, 2024

Abstract

Due to the shortening of the duration of the process and the possibility of obtaining crystals of smaller and uniform size, microwave heating is considered an effective and promising tool for the synthesis of $LiMn_2O_4$, a valuable cathode material for lithium-ion batteries. However, the electrochemical characteristics of $LiMn_2O_4$ obtained with its help are almost completely absent and do not allow for drawing a sound conclusion regarding the advantages and drawbacks of microwave processing. Here, we describe the microwave-assisted citric acid aided synthesis, characterization and electrochemical performance of $LiMn_2O_4$. The disclosure of detailed working protocols enabling one to manufacture samples tolerant to extremely high currents is the main novelty of this paper. Specifically, our material sustains current loads up to 40 C (5920 mA g^{-1}) and completely recovers after cycling in harsh conditions.

Keywords

Microwave processing; batteries; lithium manganese spinel; high-rate properties

Introduction

Thirty years after successful commercialization, lithium-ion batteries continue to conquer the world, making them increasingly independent of wired power supplies. Lithium manganese spinel $LiMn_2O_4$ belongs to a privileged group of successfully commercialized cathode materials [1]. Unlike ubiquitous $LiCoO_2$, lithium manganese spinel is cheap and non-toxic, so its application fields are being expanded steadily and have already captured the automotive industry [2].

The synthesis method plays a key role in obtaining high-performance spinels. Analysis reveals, however, that standard solid state and precipitation routes cannot provide proper electrochemical parameters [3]. The theoretical specific capacity of $LiMn_2O_4$ ($Q_{sp,theor.}$ = 148 mAh g^{-1}) is seldom attained, and the ability to sustain high current loads shows up in hard-to-reach nanostructured samples.

An idea of improving the quality of electrode materials by passing from micro- to nanosized level, first articulated by Aricò *et al.* [4], relies on the possibility of reducing the transport path of lithium ions and electrons within the electrode volume upon the subdivision of material particles, thereby augmenting their high-rate properties. This idea was involved in a huge variety of works carried out by means of sol-gel methods [5,6], spray pyrolysis [7], hydrothermal technology [8], as well as approaches inherent to nanochemistry, like self-assembly [9], template synthesis [10], *etc*. [11,12]. Most of these approaches can hardly be implemented in the near future due to their intricate nature. On the other hand, there are several easily scalable methods that look prospectively for significant enhancement of the properties of electrode materials. These are a citric acid-aided route and microwave heating, briefly discussed in what follows and constitute the subject of this work.

Oxy- and amino acid-aided routes are widely used for the synthesis of electrode materials [3,11] and have already been implemented on a small to medium-sized level [13,14]. The essence of the citric acid aided route lies in the pyrolysis of acidic metal citrates, which is strongly exothermal, involves the loss of a great amount of gaseous reaction products, and leads to oxides or their mixtures in the nanosized form. Much work has been done to optimize the synthetic conditions to obtain materials with the smallest particle size. It has been shown, in particular, that in the course of the synthesis, acidic metal citrates are forming, an optimal metal-to-acid ratio is 1:2, and additives, like ethylene glycol, are unnecessary [15,16]. This modified citric acid aided route has been employed for obtaining and detailed characterization of several electrode materials of exceptional high-rate performance [17-23].

Using microwave (MW) radiation in the synthesis of electrode materials has advantages from several viewpoints [24,25]. Due to the interactions of microwaves with particles, the heat is generated directly in the volume of a material and spreads rapidly and uniformly. First of all, this significantly reduces the duration of synthesis. Second, decreasing heat exposure time results in obtaining more finely dispersed and less agglomerated materials. This makes microwave heating an effective tool for controlling the particles' morphology. The possible use of MW heating in the manufacturing of electrode materials is favored by the widespread use of microwave ovens in industrial heating and drying applications like pharmaceutical production, food processing, crop and timber drying, *etc*.

As follows from literature sources dealing with $LiMn_2O_4$, the use of MW radiation is indeed an effective and promising method. Carrying out MW heating at various stages of solid state, sol-gel (combustion) and hydrothermal syntheses [26-43] reduces the duration of the process and promotes the formation of crystals of smaller and more uniform size. However, data on the electrochemical characteristics of such materials are either completely absent [27,28,31,35,36,42] or limited by a conclusion regarding fast capacity fade during relatively short cycling and discharge with currents up to 10 C [26,29,30,32-34,37-41,43]. The same is true for $LiMn_2O_4$ obtained by means of a citric acid aided route and MW heating [44,45]. Only very recently, $LiMn_2O_4$ synthesized in this manner has been subjected to detailed electrochemical tests [46]. It appears, however, that in spite of quite similar particle size, its high-rate properties are much worse than those of a material made with the help of conventional thermal treatment [17,20]. One may speculate that the synthetic protocol employed in [45] is far from optimal. For comparison, the electrochemical properties of $LiMn_2O_4$ spinels obtained by various synthesis methods in combination with MW heating are summarized in Table 1.

Table 1. *Electrochemical properties of $LiMn_2O_4$ spinels obtained by various MW-assisted synthesis methods*

Synthesis method	Discharge capacity, mAh g^{-1} (*C*-rate)		Capacity retention, % / *C*-rate/ cycle	Ref.
	C_{min}	C_{max}		
MW solid state	120 (0.2 C)	–	72 / 1 C / 300	[26]
MW solid state	102	–	~80 / 100	[30]
MW solid state	112 (0.25 C)	95 (1 C)	82 / 1 C / 50	[37]
MW solid state	142.5 (0.1 C)	~90 (10 C)	-	[38]
MW solid state	121 (1 C)	57 (13.5 C)	95 / 1 C / 20	[47,48]
MW combustion	112-133 (C/3)	117 (1 C)	90 / C/3 / 30	[32,33]
MW combustion	114 (1 C)	-	75 / 1 C /100	[40]
MW sol-gel	116 (0.3 C)	–	98 / 0.3 C / 30	[45]
MW combustion	120 (1 C)	~60 (10 C)	~30 / 1 C / 1000	[46]
MW rheological phase	127 (1/6 C)	117 (2/3 C)	~84 / C/3 / 40	[34]
MW co-precipitation	132 (0.2 C)	92 (10 C)	75 / 0.5 C / 100	[39]
MW hydrothermal	89 (0.14 C)	59 (1.4 C)	85 / 0.14 C / 25	[41]
MW hydrothermal	132 (0.1 C)	34 (10 C)	73 / 0.1 C / 50	[43]

In previous papers of our lab, conventional and MW-assisted solid-state routes of the synthesis of $LiMn_2O_4$ from various raw materials have been compared [47,48]. It has been found that the samples synthesized from carbonates behave better than those obtained from acetates, and microwave-heated specimens overwhelm those prepared by a conventional method. Specifically, they have $Q_{sp.}$ close to 120 mAh g^{-1} and deliver ~50 % of their initial capacity being loaded with the current of 1500 to 2000 mA g^{-1} (10-13.5 C). Here, we continue this work and present a description of the synthesis, characterization and electrochemical performance of $LiMn_2O_4$ obtained by means of microwave-assisted citric acid aided route. The combination of this synthesis technique with MW heating makes it possible to significantly reduce the particle size compared to the previously used MW-assisted solid-state method, which positively affects the kinetic characteristics of $LiMn_2O_4$. The disclosure of detailed working protocols enabling one to manufacture samples faster, sustaining the currents that exceed 5900 mA g^{-1} (~40 C) is the main novelty of this paper.

Experimental

Reagents and MW synthesis

Solutions of lithium nitrate, manganese nitrate and citric acid were prepared from analytical grade LiOH, HNO_3, $Mn(NO_3)_2{\cdot}6H_2O$, and $C_6H_8O_7{\cdot}H_2O$ (Makrokhim, Ukraine). To ensure twofold excess of the acid over the sum of metals, 60 ml of 0.5 M $LiNO_3$, 60 ml of 1 M $Mn(NO_3)_2$ and 90 ml of 2 M $C_6H_8O_7$ solutions were mixed and subjected to stirring on a magnetic stirrer for 15 to 30 min. The total volume of the working solution for a batch subjected to MW irradiation was 30 ml. MW synthesis was performed in household Saturn ST-MW7154 (Czech Republic) and LG MS-1949W (Korea) MW ovens with radiation frequency of 2.45 GHz and maximal power of 700 W. The MW radiation power was set in the range from 120 to 700 W, depending on the stage of synthesis, which is described in more detail below. Temperature measurement was carried out by means of a UT303A contactless infrared pyrometer after temporarily switching the furnace off. The final annealing was performed in a muffle furnace in the air for 24 h at 700 °C with heating and cooling rates of 5 and 2 °C min^{-1}, respectively. All operations were executed in alumina or thermal glass beakers. A flowchart of the synthesis is presented in Scheme 1.

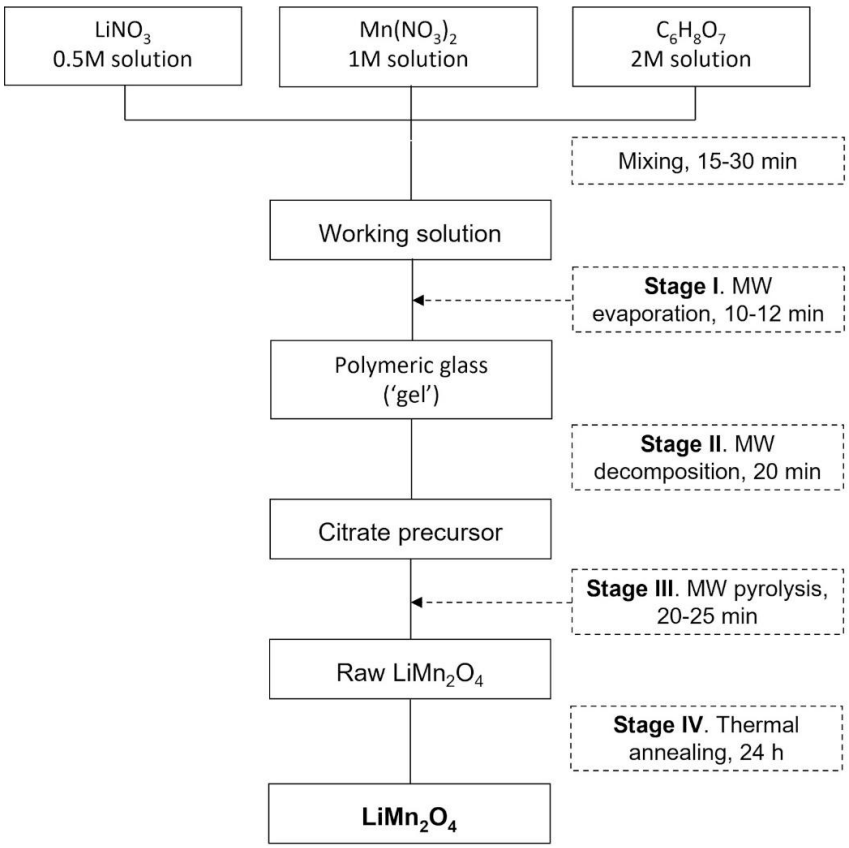

Scheme 1. *Flowchart of citric acid aided MW synthesis of $LiMn_2O_4$*

Characterization

X-ray diffraction (XRD) measurements were made on a LOMO DRON-4-07 X-ray diffractometer (Russia) with Cu-K_α (λ = 0.15418 nm) radiation. Crystallite size was calculated using the Scherrer equation. Scanning electron micrographs (SEM) were taken on a JEOL JSM 6700F microscope (Japan). Surface area and porosity were measured on a Micromeritics ASAP 2000 device (USA).

Electrochemical tests

Electrochemical testing was carried out on a homemade automatic workstation in 2016 coin cells with lithium anode. The slurry containing 80.6 % of $LiMn_2O_4$, 11.4 % of a conducting additive (5 % SFG-6 and 6.4 % Super P, both Timcal) and 8 % of a binder (PVDF, Kureha) was cast on an aluminum foil by a doctor blade with a gap of 125 µm. A Celgard 2500 separator (Switzerland) of 25 µm thickness was employed. The mass load of $LiMn_2O_4$ was in the range of 4.4-5.2 mg cm^{-2}. Before cell assembling, electrodes were dried at 120 °C for 15 h in a vacuum. 1M solution of $LiPF_6$ in a mixture of ethylene carbonate and dimethyl carbonate (1:1 by mass, Aldrich, USA) served as electrolyte. Galvanostatic measurements were performed within the 3.4-4.5 V potential range employing a constant current - constant voltage (CCCV) charge mode. Current densities were measured in C-rate values based on the theoretical specific capacity of $LiMn_2O_4$ (1 C = 148 mA g^{-1}). Cyclic voltammetric (CV) curves were registered within the same voltage limits at 0.1 mV s^{-1} sweep rate.

Results and discussion

MW synthesis

The known scheme of a citric acid aided route consists of the following stages [11,15,16]. Evaporating solutions containing a metal nitrate and citric acid, one obtains glassy hydrous acidic

citrates, including nitric acid. Decomposing these glasses leads to precursors of hydrous acidic citrates in the form of sponge-like cakes. Pyrolysis of the precursors and (optionally) further annealing of pyrolysis products gives target oxides. All these stages are well distinguishable in MW synthesis.

The removal of water (stage I) and the formation of a citrate precursor (stage II) can be performed continuously. Stage I has been carried out at a radiation power of 260 W. The process lasts for 10 to 12 min; the viscosity of the solution grows, and emission centers of a brown gas (NO_2) appear on the surface, signifying that the displacement of nitric acid by citric acid begins and the formation of a citrate precursor starts. To decrease gas evolution rate, the radiation power must be reduced to 120 W for 5 min. For complete removal of nitrous oxides, further heating at 460 W for 5 min and at 600 W for 10 min. is required. At these conditions, the main part of gaseous products is removed and the citrate precursor is obtained in the form of the so-called sponge-like cake.

The pyrolysis of citrate precursors (stage III) is known to be a stepwise process involving (i) endothermic dehydration of a hydrous salt and decomposition of citrate anion to the anions of (ii) aconitic and (iii) citraconic acid and then to (iv) citraconic anhydride, whose breakdown (v) occurs exothermically. Performing stage III requires a radiation power of 700 W. At the initial stage, heating occurs quickly, and dehydration ends in 2 to 2.5 min at ~150 to 200 °C. In cases where a reaction product rises, it has to be deflated by punching down with a spatula. Further heating is slow and 15 to 20 min elapse until exothermic reaction begins. Its onset is marked by releasing an acrid smoke, changing the color of the reaction product to black. Then it becomes red hot (Figure 1) and sometimes an open flame appears. At this moment, the product has either been removed from the oven or subjected to MW post-heating at 420 W for 2 or 4 min. In the former case, the mean temperature equals 450 to 520 °C (at the peak moment of combustion, the temperature exceeds 600 °C) and visually, burning is self-propagating. Such a wide range of temperatures is associated with a change in the amount of heat released during the gradual propagation of combustion. In the latter cases, the mean temperature is the same, and the maximal temperature exceeds 650 °C. In this case, the higher temperature is associated with the simultaneous combustion of the precursor and the heating under the MW radiation of the oxide phase formed. Hereinafter, the samples are marked MW-0 (without MW post-heating), MW-2 (MW post-heating at 420 W for 2 min) and MW-4 (MW post-heating at 420 W for 4 min).

Figure 1. *Burning of a citrate precursor*

All these operations last for maximally 1 h in total and occur at least twice as shorter as at common heating. The synthesis was completed by prolonged annealing (stage IV) in a muffle furnace at the temperature of 700 °C, as indicated in the Experimental section.

Characterization

To understand how thermal treatment influences the parameters of materials, we have compared diffractograms of pyrolyzed products at different stages. As follows from Figure 2a, $LiMn_2O_4$ is directly forming from acidic citrates of manganese and lithium at Stage III just after burning and before MW post-heating at 420 W, this is evidenced by the presence of reflections from its (111), (311), (222), (400), (331), (511), (440) i (531) crystallographic planes. During this time, however, a great number of Mn_3O_4 admixtures are accumulated. Continuing MW treatment (post-heating) at Stage III and performing annealing at 700 °C for 24 h (stage IV), one obtains single-phase $LiMn_2O_4$ with no admixtures (Figure 2b-d).

Lattice parameters (*a*) and volumes (*V*), as well as crystallite sizes (d_{400}) determined using the reflection from the (400) plane for MW-0, MW-2 and MW-4 samples, are collected in Table 2. It is seen that all samples are commensurable by lattice parameters, volumes, and crystallite sizes, so the variation of residence time upon MW treatment does not influence these values. On the other hand, comparing *a*, *V* and d_{400} for our samples and materials synthesized by means of MW-assisted solid state reaction [47,48], one reassures that the latter leads to more dense specimens.

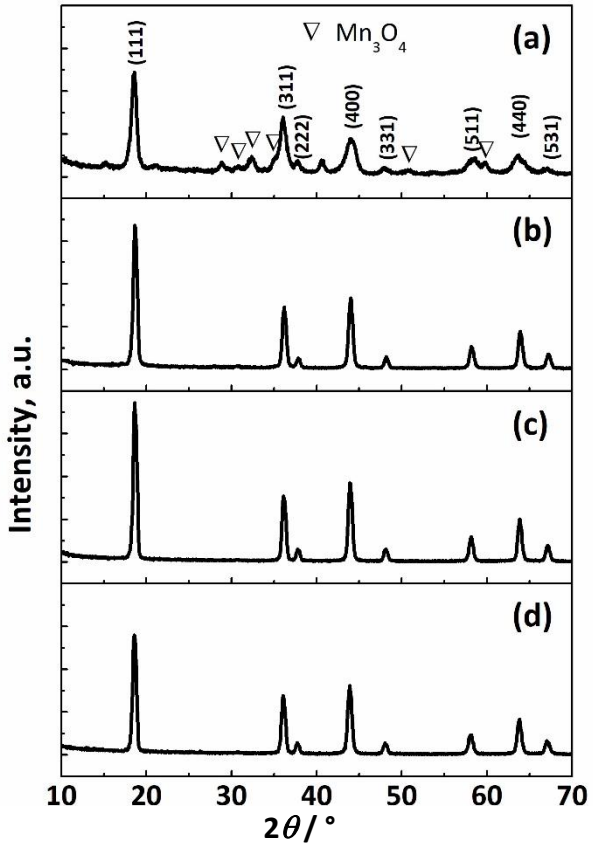

Figure 2. *XRD patterns of $LiMn_2O_4$ just after burning and before MW post-heating at 420 W (a), and after MW post-heating at 420 W and annealing at 700 °C for 24 h (b) MW-0, (c) MW-2, (d) MW-4. Peak indexing corresponds to JCPDS 35-782 ($LiMn_2O_4$) and 24-0734 (Mn_3O_4)*

SEM data for our samples are presented in Figure 3. Here, one can follow the influence of both MW-post-heating (stage III) and annealing (stage IV) on the sample morphology. $LiMn_2O_4$ taken just after burning has a particle size of less than 50 nm (Figure 3a). Further annealing at 700 °C for 24 h

causes expected particle enlargement to 50-60 nm size (Figure 3b). Interestingly, the samples were subjected to the MW post-heating for 2 and 4 min, and annealing increased their size to 100-120 nm (Figure 3c, d). For the same samples, the particles are more perfect (the edges of the faces of the crystals characteristic of the $LiMn_2O_4$ octahedral shape are clearer), which is evidence of the higher crystallinity of these samples. This observation confirms that crystal growth, sintering and recrystallization are much faster upon MW treatment. In our case, the particle size doubles upon MW heating at 420 W for 4 min. Given this, more prolonged MW post-heating was not performed to avoid further growth of particle size.

Porosimetric studies signify that the samples obtained are non-porous. This is common for spinels [16,17]. It appears that the MW-post-heating significantly decreases both specific surface area ($S_{sp.}$) and pore volume (V_{pore}) (Table 2). Such observation is consistent with SEM data and probably results from compaction upon sintering.

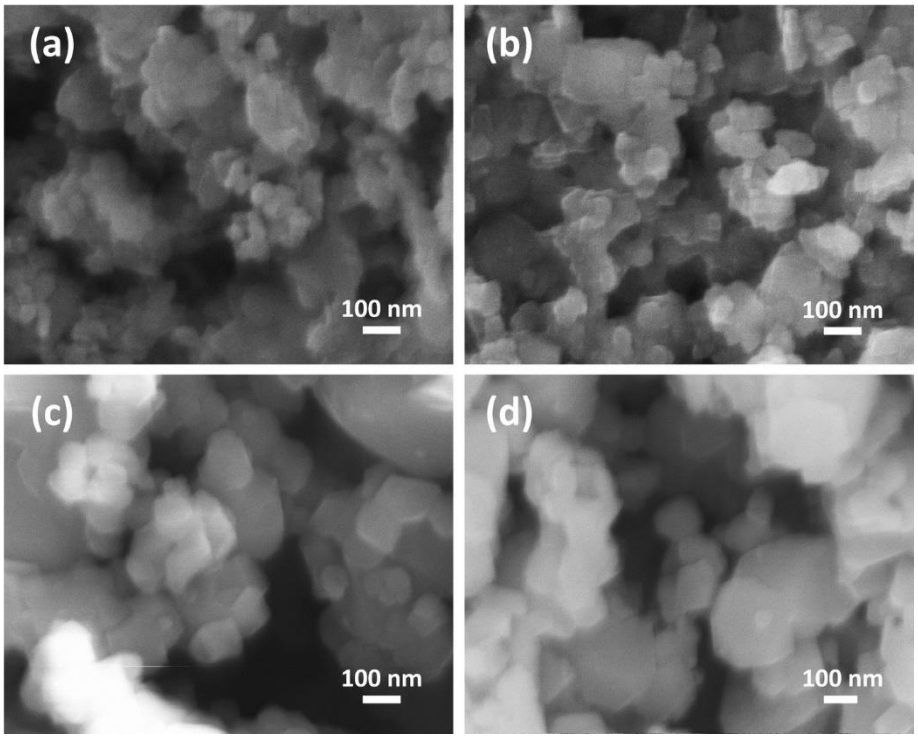

Figure 3. *SEM micrographs of $LiMn_2O_4$ just after burning and before MW post-heating at 420 W(a), and after MW post-heating at 420 W and annealing at 700 °C for 24 h (b) MW-0, (c) MW-2, (d) MW-4*

Table 2. *Parameters of various $LiMn_2O_4$ samples*

Sample	a / nm	V / nm^3	d_{400} / nm	Particle size, nm	S_{sp} / m^2 g^{-1}	V_{pore} / cm^3 g^{-1}
MW-0	0.8195	0.550	17	50	13.3	0.147
MW-2	0.8204	0.552	18	100	5.4	0.048
MW-4	0.8212	0.554	18	120	5.4	0.047

Electrochemical tests

Figure 4a-c shows the first three charge/discharge cycles for MW-0, MW-2 and MW-4 samples. All these curves have a typical form demonstrating two plateaus corresponding to equilibria between $LiMn_2O_4$ and an intermediate $Li_{0.5}Mn_2O_4$ and between the latter and MnO_2. In all cases, a solid electrolyte interface forms at the first charge, causing a great excess of charge capacity over discharge capacity: Coulombic efficiencies measured as $CE = Q_{sp,\ discharge}/Q_{sp,\ charge}$ ratio do not exceed 86 %. Upon 2nd and 3rd cycles, these become close to 100 %. The specific capacities of MW-0, MW-2 and MW-4

samples on the 3rd cycle appear equal to 85, 97 and 90 mAh g^{-1}. In general, the specific capacity of spinels is often significantly lower than the theoretical value, which is a typical phenomenon for this electrode material [3]. For example, in conventional citrate syntheses of $LiMn_2O_4$, the best $Q_{sp.}$ obtained is 110 mAh g^{-1} [20]. In our case, a significant part of lithium ions (about a third of the theoretical content) is unavailable for certain reasons and does not participate in the electrochemical process at all. However, it should be noted that during the combined CCCV charge mode, the share of the capacity obtained in the constant voltage mode is small compared to the capacity in the constant current mode, which indicates a sufficiently high mobility of the lithium ions available for the electrochemical process. The same conclusion follows from the shape of cyclic voltammetry (CV) curves (Figure 4d). The CV curves of MW-2 and MW-4 samples have two distinct peaks corresponding to the intercalation/deintercalation of lithium ions in the spinel structure. These samples are close to each other and are characterized by higher peak intensities than the MW-0 sample. In the latter case, the peaks are practically not split and shifted to higher potentials during charge and to lower potentials during discharge due to polarization. According to the data presented in Table 3, the difference between the corresponding CV peaks ΔE_1 and ΔE_2 in the case of MW-2 and MW-4 samples is actually half as much as compared to MW-0 sample. CV data registered for MW-2 and MW-4 samples suggest their lower current resistance and better kinetics of charge/discharge processes.

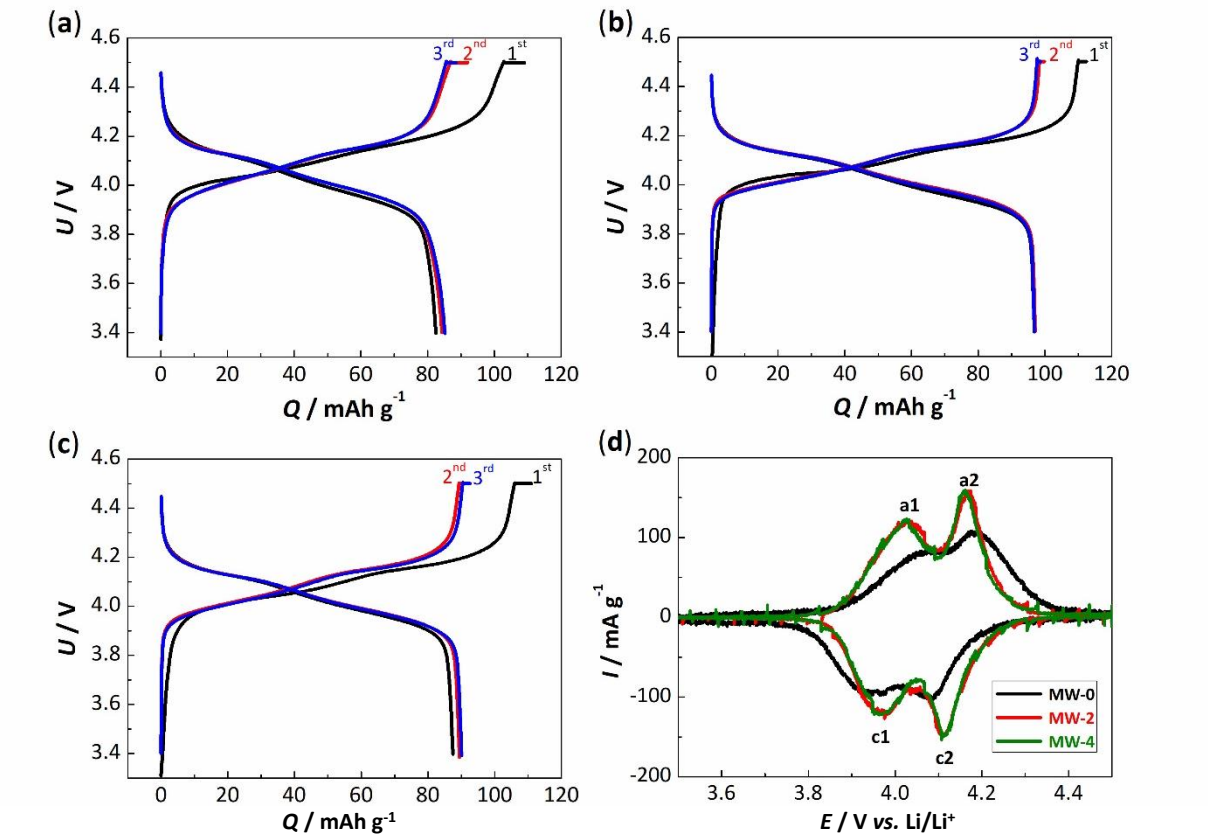

Figure 4. *Charge/discharge curves for (a) MW-0, (b) MW-2 and (c) MW-4 samples at cycling current 0.5 C and tapered current on charging 0.1 C, (d) CV curves at potential sweep rate 0.1 mV s^{-1}*

Table 3. *Peak parameters of CV curves for various $LiMn_2O_4$ samples*

Sample	E_{a1} / V	E_{a2} / V	E_{c1} / V	E_{c2} / V	ΔE_1 / mV	ΔE_2 / mV
MW-0	4.076	4.186	3.955	4.085	121	101
MW-2	4.029	4.170	3.966	4.110	63	60
MW-4	4.023	4.160	3.969	4.115	54	45

Figure 5 shows the results of cycling of $LiMn_2O_4$ samples at the current density of 1 C for 100 cycles. As can be seen, the stability of the specific capacity during cycling increases with an increase in the duration of the MW post-heating. The initial discharge capacity at 1 C is almost identical to that obtained at the current density of 0.5 C and is 85, 96, and 90 mAh g^{-1} for samples MW-0, MW-2, and MW-4, respectively. The values of the specific capacity obtained after 100 cycles for samples MW-0, MW-2 and MW-4 are 73, 94, and 90 mAh g^{-1}, respectively, which corresponds to capacity retention (CR) of 86, 97, and 100 %. Thus, sample MW-4 demonstrates excellent cycling stability despite a slightly lower specific capacity than sample MW-2.

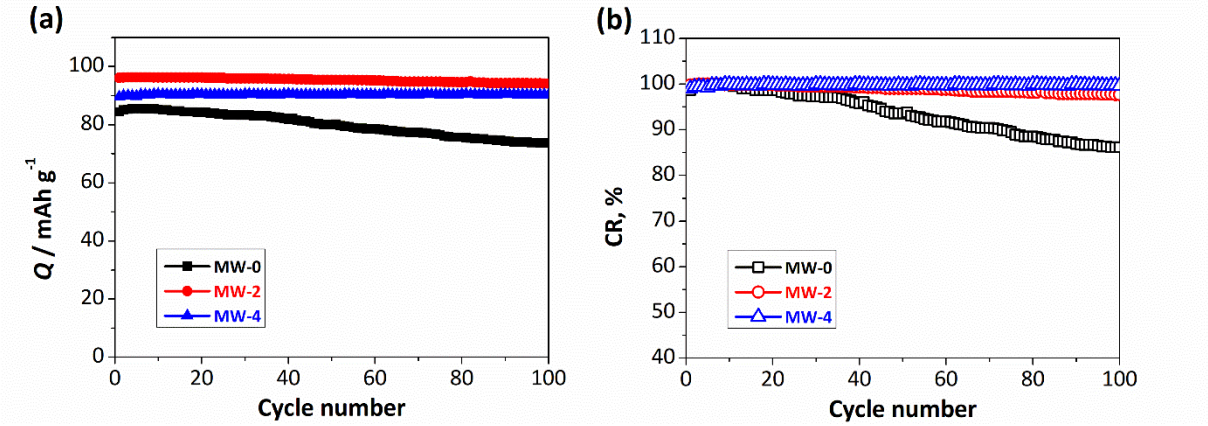

Figure 5. *Cycling performances of $LiMn_2O_4$ samples at the current density of 1 C: dependence of discharge capacity on cycle number (a), and capacity retention curves (b)*

High-rate testing results are presented in Figure 6. It turns out that the ability to sustain high-rate current loads is better for the samples subjected to longer MW post-heating. The MW-0 material, which has not been MW post-heated, quickly loses its capacity upon a 6 C current load and, at a 12 C rate, delivers 25 mAh g^{-1} (Figure 6a). The MW-2 sample MW post-heated for 2 min is more stable and delivers the same capacity at ~25 C rate. The best results are demonstrated by the MW-4 sample sustaining current loads up to 40 C (5920 mA g^{-1}) and returning 20 mAh g^{-1} at this current rate. Furthermore, after cycling at such harsh conditions (up to 80 C, *i.e.*, 11840 mA g^{-1} for MW-2) and returning to discharge by low currents, all samples completely retain their initial capacity (see control cycles by 1 C current in Figure 6a-c). This suggests that the obtained samples do not actually degrade in the range of 50-100 cycles.

In Figure 6d, we compare the high-rate abilities of all three synthesized samples, plotting capacity retention determined as CR / %= $Q_{sp.}(C)/Q_{sp.\ max.}$ *vs.* C-rates. This plot shows that the capacity retention significantly grows with increasing the MW post-heating time. For spinels post-heated for 0, 2 and 4 min, half of the initial capacity is delivered upon current load of 9, 19.5 and 26.5 C. This is significantly higher than for the best samples obtained by means of MW solid-state [47,48] and MW co-precipitation [39] routes, as well as for the spinels synthesized by conventional solid-state [49] and co-precipitation [50] techniques in recent five years. At the same time, it should be noted that the nominal specific capacity obtained at low discharge rates is higher when using both MW and traditional solid-state and co-precipitation synthesis techniques. If the $LiMn_2O_4$ obtained by the citric acid aided route with MW heating and the conventional time-consuming citric acid aided route are compared [17,20], in both cases, the closeness of the specific capacities, as well as the maximum discharge rates (up to 40 C). Taking this into account, the obvious advantage of MW heating is its short duration, which allows it to significantly intensify the entire synthesis process without losing the functional properties of the material.

Interestingly, the results of existing high-rate tests of $LiMn_2O_4$ synthesized in a similar way (microwave-assisted citric acid aided route) [46] are quite close to our data obtained without post-heating and are significantly inferior to those attained for MW-2 and MW-4 samples, see Figure 5d. This clearly shows that MW post-heating is advantageous for improving the electrochemical performance of lithium-manganese spinels, *i.e.*, apparently, small action greatly affects the properties of a material.

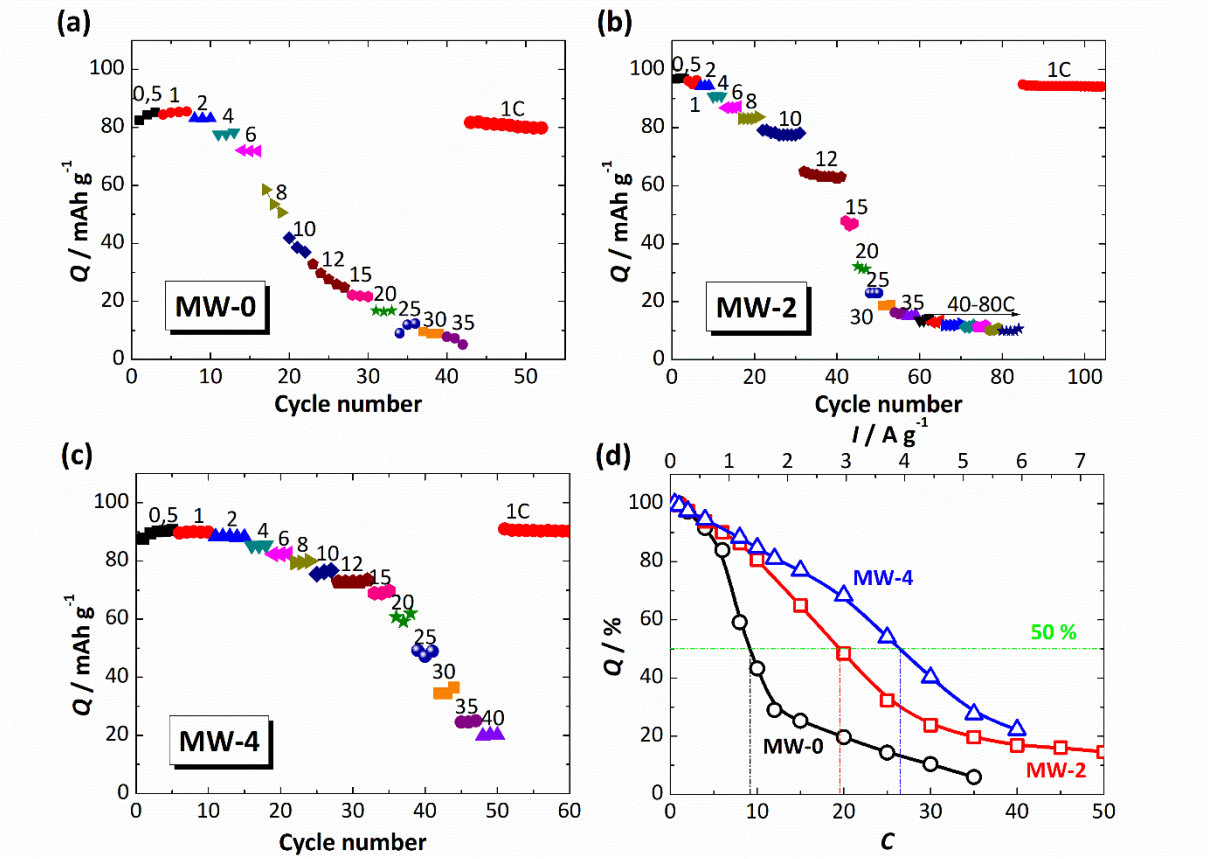

Figure 6. *Dependences of specific capacity at various current loads on cycle number for MW-0 (a), MW-2 (b) and MW-4 (c) samples, and of capacity retention on current rate (d). Charge current 1 C with tapered current 0.1 C. Figures at points in (a-c) panels denote current C-rates*

Conclusions

In this paper, we have presented an in-depth description of the synthesis, characterization and electrochemical performance of $LiMn_2O_4$ obtained by means of the microwave-assisted citric acid aided route. Detailed working protocols are disclosed, enabling one to reproduce this work completely and to manufacture spinels that sustain current loads at least two times as high as common heating methods. Like in the case of conventional citrate synthesis, the best-synthesized samples sustain current loads up to 40 C (5920 mA g^{-1}) and completely recover after cycling at harsh conditions. Compared with samples obtained by microwave-assisted solid-state routes, our materials are much superior in high-rate properties. All microwave-assisted operations last for maximally 1 h in total and occur at least twice as shorter than at common heating. It is found that microwave post-heating of the reaction mixture after its exothermal decomposition is crucial for obtaining a high-rate cathode material.

References

[1] M. M. Thackeray, E. Lee, B. Shi, J.R. Croy, Review-from $LiMn_2O_4$ to partially-disordered Li_2MnNiO_4: the evolution of lithiated-spinel cathodes for Li-ion batteries, *Journal of The Electrochemical Society* **169** (2022) 020535. https://doi.org/10.1149/1945-7111/ac50dd.

[2] G. E. Blomgren, The development and future of lithium ion batteries, *Journal of The Electrochemical Society* **164** (2017) A5019-A5025. https://doi.org/10.1149/2.0251701jes

[3] A. V. Potapenko, S. A. Kirillov, Lithium manganese spinel materials for high-rate electrochemical applications, *Journal of Energy Chemistry* **23** (2014) 543-558. https://doi.org/10.1016/S2095-4956(14)60184-4

[4] A. S. Aricò, P. Bruce, B. Scrosati, J. M. Tarascon, W. Schalkwijk, Nanostructured materials for advanced energy conversion and storage devices, *Nature Materials* **4** (2005) 366-377. https://doi.org/10.1038/nmat1368

[5] Z. Zhang, B. McNall, A. B. Kanagaraj, J. R. Park, J. E. Ryu, D. Choi, Electrochemical characterization of $LiMn_2O_4$ nanowires fabricated by sol-gel for lithium-ion rechargeable batteries, *Materials Letters* **273** (2020) 127923. https://doi.org/10.1016/j.matlet.2020.127923

[6] A. M. Hashem, A. E. Abdel-Ghany, H. M. Abuzeid, R. S. El-Tawil, S. Indris, H. Ehrenberg, A. Mauger, C. M Julien, EDTA as chelating agent for sol-gel synthesis of spinel $LiMn_2O_4$ cathode material for lithium batteries, *Journal of Alloys and Compounds* **737** (2018) 758-766. https://doi.org/10.1016/j.jallcom.2017.12.153

[7] R. Kun, P. Schlee, E. Pal, M. Busse, T. Gesing, Role of the precursor chemistry on the phase composition and electrochemical performance of thin-film $LiMn_2O_4$ Li-ion battery cathodes prepared by spray pyrolysis. *Journal of Alloys and Compounds* **726** (2017) 664-674. https://doi.org/10.1016/j.jallcom.2017.08.039

[8] H. Gao, Q. Yan, P. Xu, H. Liu, M. Li, P. Liu, J. Luo, Z. Chen, Efficient direct recycling of degraded $LiMn_2O_4$ cathodes by one-step hydrothermal relithiation. *ACS Applied Materials & Interfaces* **12** (2020) 51546-51554. https://doi.org/10.1021/acsami.0c15704

[9] W. B. Hua, S. N. Wang, X. D. Guo, S. L. Chou, K. Yin, B. H. Zhong, S. X. Dou, Vacuum induced self-assembling nanoporous $LiMn_2O_4$ for lithium ion batteries with superior high rate capability, *Electrochimica Acta* **186** (2015) 253-261. https://doi.org/10.1016/j.electacta.2015.10.093.

[10] S. Chen, Z. Chen, C. Cao, Mesoporous spinel $LiMn_2O_4$ cathode material by a soft-templating route, *Electrochimica Acta* **199** (2016) 51-58. https://doi.org/10.1016/j.electacta.2016.03.135.

[11] S. A. Kirillov, Electrode materials and electrolytes for high-rate electrochemical energy systems: a review, *Theoretical and Experimental Chemistry* **55** (2019) 73-95. https://doi.org/10.1007/s11237-019-09598-2.

[12] A. H. Marincaş, F. Goga, S. A. Dorneanu, P. Ilea, Review on synthesis methods to obtain $LiMn_2O_4$-based cathode materials for Li-ion batteries, *Journal of Solid State Electrochemistry* **24** (2020) 473-497. https://doi.org/10.1007/s10008-019-04467-3

[13] C. Bluthardt, C. Fink, K. Flick, A. Hagemeyer, M. Schlichter, A. Volpe Jr, Aqueous synthesis of high surface area metal oxides, *Catalysis Today* **137** (2008) 132-143. https://doi.org/10.1016/j.cattod.2008.04.045

[14] C. Fink, A. Hagemeyer, Z. Hogan, A. Volpe Jr., J. Yoder, High surface area cerium oxide, *Current Catalysis* **5** (2016) 182-202. https://doi.org/10.2174/2211544705666160509161559

[15] I. A. Farbun, I. V. Romanova, S. A. Kirillov. Optimal design of powdered nanosized oxides of high surface area and porosity using a citric acid aided route, with special reference to ZnO, *Journal of Sol-Gel Science and Technology* **68** (2013) 411-422. https://doi.org/10.1007/s10971-013-3024-7

[16] I. V. Romanova, S. A. Kirillov, Preparation of Cu, Ni and Co oxides by a citric acid-aided route, *Journal of Thermal Analysis and Calorimetry* **132** (2018) 503-512. https://doi.org/10.1007/s10973-017-6880-5

[17] A. V. Potapenko, S. I. Chernukhin, S. A. Kirillov, A new method of pretreatment of lithium manganese spinels and high-rate electrochemical performance of $Li[Li_{0.033}Mn_{1.967}]O_4$. *Materials for Renewable and Sustainable Energy* **3** (2014) 40. https://doi.org/10.1007/s40243-014-0040-7

[18] A. V. Potapenko, S. I. Chernukhin, I. V. Romanova, K. Sh. Rabadanov, M. M. Gafurov, S. A. Kirillov, Citric acid aided synthesis, characterization, and high-rate electrochemical performance of $LiNi_{0.5}Mn_{1.5}O_4$, *Electrochimica Acta* **134** (2014) 442-449. https://doi.org/10.1016/j.electacta.2014.04.083

[19] V. V. Kosilov, A. V. Potapenko, S. A. Kirillov, Effect of overdischarge (overlithiation) on electrochemical properties of $LiMn_2O_4$ samples of different origin, *Journal of Solid State Electrochemistry* **21** (2017) 3269-3279. https://doi.org/10.1007/s10008-017-3671-7

[20] A. V. Potapenko, S. A. Kirillov, Enhancing high-rate electrochemical properties of $LiMn_2O_4$ in a $LiMn_2O_4/LiNi_{0.5}Mn_{1.5}O_4$ core/shell composite, *Electrochimica Acta* **258** (2017) 9-16. https://doi.org/10.1016/j.electacta.2017.10.108

[21] S. A. Kirillov, I. V. Romanova, T. V. Lisnycha, A. V. Potapenko, High-rate electrochemical performance of $Li_4Ti_5O_{12}$ obtained from $TiCl_4$ by means of a citric acid aided route, *Electrochimica Acta* **286** (2018) 163-171. https://doi.org/10.1016/j.electacta.2018.08.034

[22] A. V. Potapenko, M. Wu, S. A. Kirillov, Remarkable electrochemical performance of $0.5Li_2MnO_3{\cdot}0.5LiNi_{0.5}Mn_{0.3}Co_{0.2}O_2$ synthesized by means of a citric acid-aided route, *Journal of Solid State Electrochemistry* **23** (2019) 3383-3389. https://doi.org/10.1007/s10008-019-04442-y

[23] S. A. Kirillov, A. V. Potapenko, A. V. Potapenko, Effect of overdischarge (overlithiation) on electrochemical properties of $LiNi_{0.5}Mn_{1.5}O_4$ samples of different origin, *Journal of Solid State Electrochemistry* **24** (2020) 1113-1121. https://doi.org/10.1007/s10008-020-04601-6.

[24] S. Balaji, D. Mutharasu, N. S. Subramanian, K. Ramanathan, A review on microwave synthesis of electrode materials for lithium-ion batteries, *Ionics* **15** (2009) 765-777. https://doi.org/10.1007/s11581-009-0350-4.

[25] F. K. Butt, A. S. Bandarenka, Microwave-assisted synthesis of functional electrode materials for energy applications, *Journal of Solid State Electrochemistry* **20** (2016) 2915-2928. https://doi.org/10.1007/s10008-016-3315-3

[26] H. Yan, X. Huang, L. Chen, Microwave synthesis of $LiMn_2O_4$ cathode material, *Journal of Power Sources* **81-82** (1999) 647-650. https://doi.org/10.1016/S0378-7753(99)00112-3

[27] P. S. Whitfield, I. J. Davidson, Microwave synthesis of $Li_{1.025}Mn_{1.975}O_4$ and $Li_{1+x}Mn_{2-x}O_{4-y}F_y$ (x= 0.05, 0.15; y = 0.05, 0.1), *Journal of The Electrochemical Society* **147** (2000) 4476-4484. https://doi.org/10.1149/1.1394089

[28] M. H. Bhat, B. P. Chakravarthy, P. A. Ramakrishnan, A. Levasseur, Microwave synthesis of electrode materials for lithium batteries, *Bulletin of Materials Science* **23** (2000) 461-466. https://doi.org/10.1007/BF02903884

[29] H. Hao, H.-X. Liu, S.-X. Ouyang, Microwave synthesis of cathode material $Li_xMn_2O_4$ for lithium-ion battery, *Journal of Wuhan University of Technology-Material Science* **17** (2002) 36-38. https://doi.org/10.1007/BF02838413

[30] M. Nakayama, K. Watanabe, H. Ikuta, Y. Uchimoto, M. Wakihara, Grain size control of $LiMn_2O_4$ cathode material using microwave synthesis method, *Solid State Ionics* **164** (2003) 35-42. https://doi.org/10.1016/j.ssi.2003.08.048

[31] S. Kobayashi, T. Usui, H. Ikuta, Y. Uchimoto, M. Wakihara, Preparation of cathode active materials for lithium ion secondary batteries utilizing microwave irradiation: Part II. Electronic structure of lithium manganese oxide, *Journal of Materials Research* **19** (2004) 2421-2427. https://doi.org/10.1557/JMR.2004.0313

[32] Y.-P. Fu, C.-H. Lin, Y.-H. Su, J.-H. Jean, S.-H. Wu, Electrochemical properties of $LiMn_2O_4$ synthesized by the microwave-induced combustion method, *Ceramics International* **30** (2004) 1953-1959. https://doi.org/10.1016/j.ceramint.2003.12.183
[33] Y.-P. Fu, Y.-H. Su, C.-H. Lin, S.-H. Wu, Comparison of the microwave-induced combustion and solid-state reaction for the synthesis of $LiMn_2O_4$ powder and their electrochemical properties, *Ceramics International* **35** (2009) 3463-3468. https://doi.org/10.1016/j.ceramint.2009.06.027
[34] B.-L. He, W.-J. Zhou, S.-J. Bao, Y.-Y. Liang, H.-L. Li, Preparation and electrochemical properties of $LiMn_2O_4$ by the microwave-assisted rheological phase method, *Electrochimica Acta* **52** (2007) 3286-3293. https://doi.org/10.1016/j.electacta.2006.10.002
[35] S. Balaji, S. Shanmugan, D. Mutharasu, K. Ramanathan, Structural, morphological and electrochemical characterization of electron beam deposited $Li_{1+x}Mn_2O_4$ (x = 0, 0.05) thin films, *Materials Science-Poland* **28** (2010) 583-593.
[36] D. Huo, Nanostructured morphology of spinel $LiMn_2O_4$ oxide under microwave heating, *Advanced Materials Research* **936** (2014) 452-458. https://doi.org/10.4028/www.scientific.net/AMR.936.452
[37] J. P. Silva, S. R. Biaggio, N. Bocchi, R. C. Rocha-Filho, Practical microwave-assisted solid-state synthesis of the spinel $LiMn_2O_4$, *Solid State Ionics* **268** (2014) 42-47. https://doi.org/10.1016/j.ssi.2014.09.025
[38] H. Zhang, Y. Xu, D. Liu, X. Zhang, C. Zhao, Structure and performance of dual-doped $LiMn_2O_4$ cathode materials prepared via microwave synthesis method, *Electrochimica Acta* **125** (2014) 225-231. https://doi.org/10.1016/j.electacta.2014.01.102
[39] X. Liu, P. Liu, H. Wang, Preparation of spinel $LiMn_2O_4$ with porous microscopic morphology by simple coprecipitation-microwave synthesis method, *Ionics* **25** (2019) 5213-5220. https://doi.org/10.1007/s11581-019-03072-8
[40] L. Tian, C. Su, Y. Wang, B. Wen, W. Bai, J. Guo, Electrochemical properties of spinel $LiMn_2O_4$ cathode material prepared by a microwave-induced solution flameless combustion method, *Vacuum* **164** (2019) 153-157. https://doi.org/10.1016/j.vacuum.2019.03.011
[41] P. Ragupathya, H. N. Vasana, N. Munichandraiah, Microwave driven hydrothermal synthesis of $LiMn_2O_4$ nanoparticles as cathode material for Li-ion batteries, *Materials Chemistry and Physics* **124** (2010) 870-875. https://doi.org/10.1016/j.matchemphys.2010.08.014
[42] M. Michalska, L. Lipińska, R. Diduszko, M. Mazurkiewicz, A. Małolepszy, L. Stobinski, K.J. Kurzydłowski, Chemical syntheses of nanocrystalline lithium manganese oxide spinel, *Physica Status Solidi C* **8** (2011) 2538-2541. https://doi.org/10.1002/pssc.201001195
[43] B. N. Rao, P. Muralidharan, P. R. Kumar, M. Venkateswarlu, N. Satyanarayana, Fast and facile synthesis of $LiMn_2O_4$ nanorods for Li ion battery by microwave assisted hydrothermal and solid state reaction methods, *International Journal of Electrochemical Science* **9** (2014) 1207-1220.
[44] H. Liu, C. Hu, X. Zhu, H. Hao, J. Luo, J. Zhou, S. Ouyang, Solid chemical reaction in microwave and millimeter-wave fields for the syntheses of $LiMn_2O_4$ compound, *Materials Chemistry and Physics* **88** (2004) 290-294. https://doi.org/10.1016/j.matchemphys.2004.06.037
[45] S.-J. Bao, Y.-Y. Liang, H.-L. Li, Synthesis and electrochemical properties of $LiMn_2O_4$ by microwave-assisted sol-gel method, *Materials Letters* **59** (2005) 3761-3765. https://doi.org/10.1016/j.matlet.2005.07.012
[46] R. Chen, B. Wen, C. Su, W. Bai, J. Guo, Significant improvement of $LiMn_2O_4$ cathode capacity by introducing trace Ni during rapid microwave-induced solution combustion, *Electrochemistry* **88** (2020) 532-539. https://doi.org/10.5796/electrochemistry.20-00083
[47] N. I. Globa, Yu. V. Shmatok, V. D. Prisyazhnyi, Structural and electrochemical characteristics of $Li_xMn_2O_4$ spinel synthesized using a microwave-assisted method, *Surface Engineering and Applied Electrochemistry* **49** (2013) 488-492. https://doi.org/10.3103/S1068375513060094

[48] N. I. Globa, Y. V. Shmatok, V. D. Prisyazhnyi, Comparison of the characteristics of $Li_xMn_2O_4$ synthesized by microwave and solid-state methods, *ECS Transactions* **48** (2014) 123-127. https://doi.org/10.1149/04801.0123ecst

[49] J. Cao, S. Guo, R. Yan, C. Zhang, J. Guo, P. Zheng, Carbon-coated single-crystalline $LiMn_2O_4$ nanowires synthesized by high-temperature solid-state reaction with high capacity for Li-ion battery, *Journal of Alloys and Compounds* **741** (2018) 1-6. https://doi.org/10.1016/j.jallcom.2018.01.107

[50] W. Zhang, Z. Zhao, Y. Lei, J. Xing, X. Cao, A facile and eco-friendly approach to synthesis of spinel $LiMn_2O_4$ with high electrochemical performance, *International Journal of Electrochemical Science* **15** (2020) 6188-6197. https://doi.org/10.20964/2020.07.77